PHY 415 Project

Gravitation Wave Detection Using Pulsar Timing Arrays

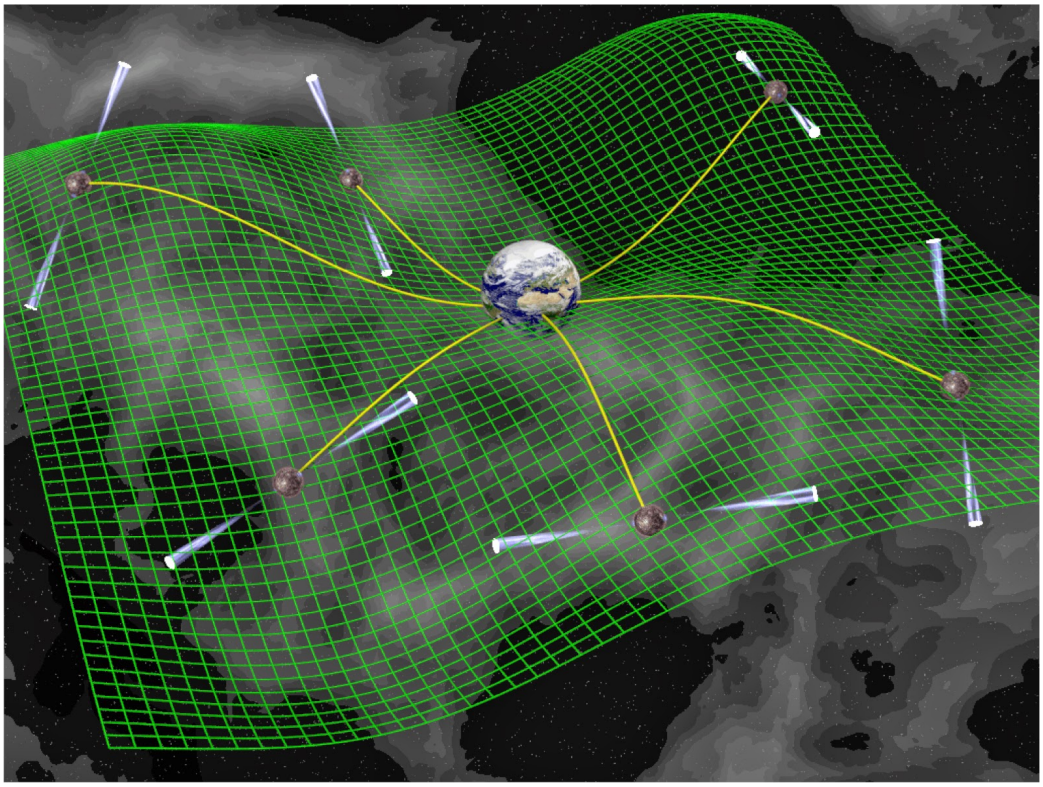

Submitted by
Pratik Manwani

Contents

List of Figures

Chapter 1

Introduction

The subject of this report is to give a broad insight into how pulsar timing works and the how it can be used to detect gravitational waves. The topic of gravitational detection is currently of great interest after the detection of gravitational waves by the LIGO collaboration. Pulsar Timing arrays offer a new possibility of detecting gravitational radiation primarily in the nano-hertz region. Pulsars are the most precise astronomical clocks and these clocks can be used to detect gravitational perturbations. These pulsar timing arrays are poised to make their detection of gravitational waves in the next five years.

The extreme environment provided by the density of pulsars allows us to use them for tests of general relativity. An indirect test of gravitational waves was performed by precise timing of Hulse-Taylor pulsar as its binary motion was in full agreement with the theoretical predictions. A more direct approach for detecting gravitational waves is to detect the gravitational waves by careful observation of the received electromagnetic pulses from the pulsars. A correlation between the pulse arrival times of different pulsars can then be formed. The gravitational waves change the time of arrival of these pulses by a few nanoseconds and this can be detected owing to stability of these pulsar clocks. However this is not a trivial task because pulsar timing is a complicated process and requires various data analysis techniques. The approach to gravitational wave detection using these pulsars and some of the approaches to pulsar timing will be discussed in this report.

Chapter 2

Pulsars

Pulsars are the strangest objects that we know about in the universe and have the most extreme physical characteristics. A pulsar is a remnant of the collapsed core of a massive star belonging to the main sequence. The fusion reactions happening in the core of a star produce heat and pressure that balances the star against gravitational collapse. Near the end of the star's life, the core runs out of fuel required for the fusion reactions and the star collapses into a small size very rapidly. The outer layers are thrown into space by a gigantic explosion which is known as the supernova. The original star collapses into a neutron star only if the mass of the original star is in the right range- about eight to twenty solar masses. The compressed core typically has a radius of about 20 kilometres but has masses about twice of that of the sun. They are the densest and smallest stars known to exist. As the star is compressed, its rotation rate increase due to the conservation of angular momentum. Because of this, the neutron stars spin very rapidly and have rotation speeds of up to hundred times per second. They also have very strong magnetic fields and due to the rotation of these fields, a powerful thin beam of electromagnetic radiation is produced that shoots into space as shown in figure 1. In general, the direction of the beam is not along the same axis as the pulsar is spinning on as shown in figure 1. So as the pulsar rotates, the beam of radiation points to different directions in the sky. If the pulsar is oriented in the right way, we get a periodic signal owing to this sweeping motion. This periodic motion is very precise and we can measure them very accurately. There are about 2000 pulsars that have been detected in total. The details of how pulsar timing works will be discussed later in the report. The pulsars used in pulsar timing arrays are of a special kind known as millisecond pulsars.

2.1 Millisecond Pulsars

Milliseconds pulsars are pulsars that have a rotation period of 1- 10 milliseconds. The leading theory that astronomers have concluded is that these objects must have an increased rate of rotation due to the accretion of material

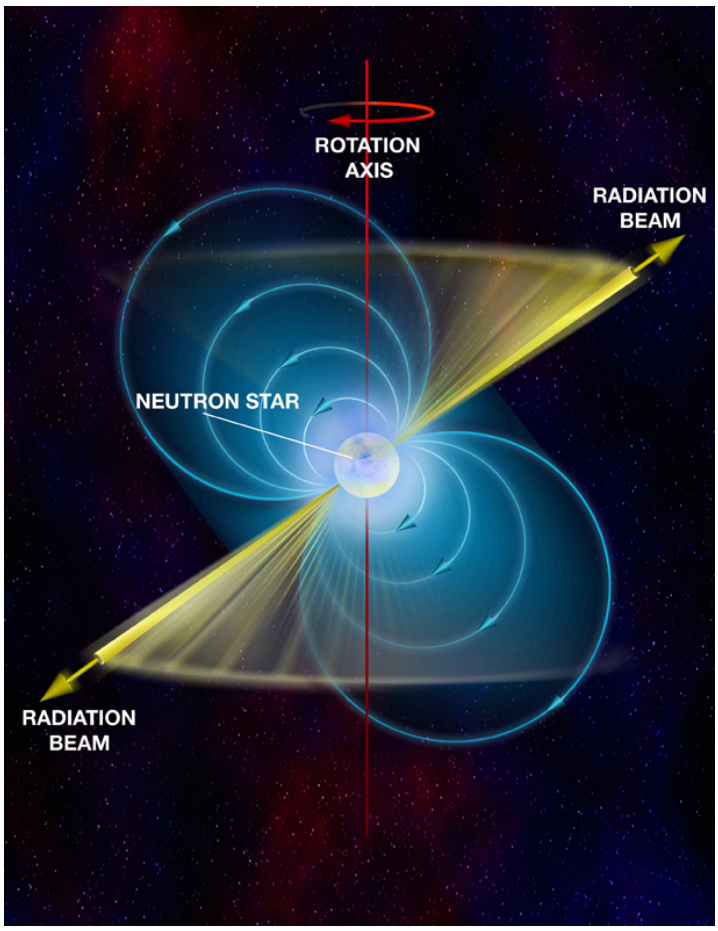

Figure 2.1: Diagram of pulsar showing beam of electromagnetic radiation and magnetic field lines, along with the axis of rotation

from a secondary star as shown in figure 2. The more massive star(primary) exhausts its main hydrogen supply and leaves a dense helium core. The primary evolves off the main sequence and begins to expand rapidly which in turn triggers mass transfer to the secondary star. This phase of mass transfer terminates when the primary's hydrogen envelope has been transferred to second. Now the secondary's mass exceeds that of the primary. The primary continues to go through the process of core burning until it reaches the iron element after which evolution stops. Gravitational collapse ensues as a result undergoing a supernova explosion and leaves behind a neutron star. If the system survives the supernova, the resulting binary consists of a high mass secondary burning core hydrogen. The expelled material of the secondary is accreted by the primary. The accretion of this matter from the secondary can spin up the neutron star, recycling it into a millisecond pulsar. The rotation increase is due to the transfer of angular momentum from the accreted matter. Millisecond pulsars can be timed with high precision and are more stable than that of normal pulsars. This is the reason why these millisecond pulsars are of great importance in pulsar timing arrays.

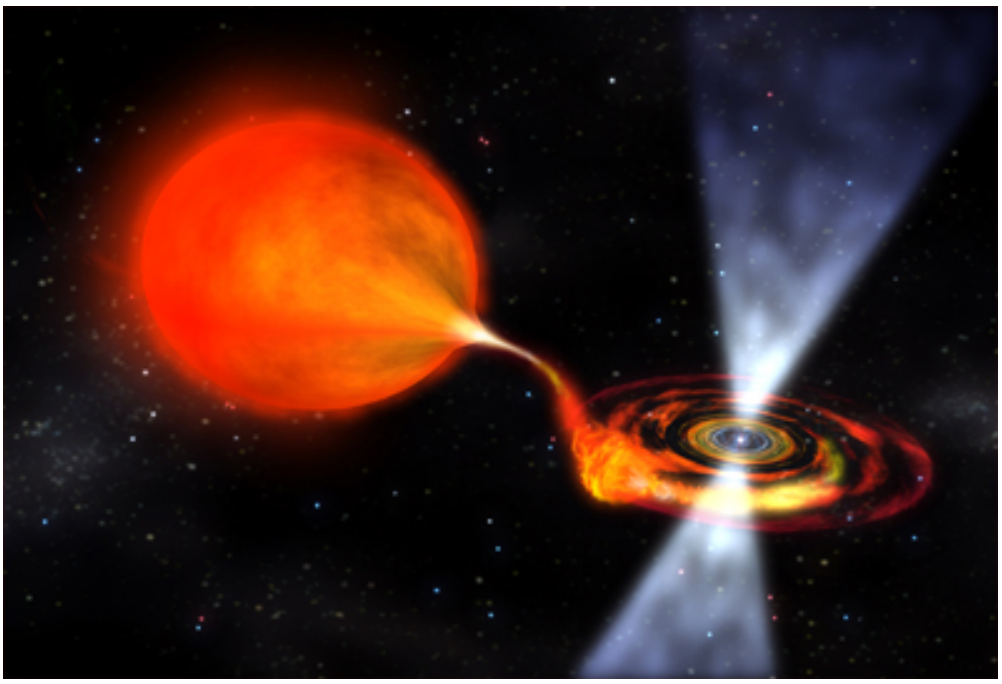

Figure 2.2: The accretion of matter from a secondary star by a neutron star

2.2 Pulse Times of Arrival (TOA)

The first step in the data analysis of the pulsar timing arrays would be to develop a method to measure the pulses and generate a pulse time of arrival. This would essentially be a timestamp on the arrival of pulses from a given pulsar. Repeated observation and study of these pulsars leads to a catalogue of their arrival times. Observations are made over many years with a sampling interval of some weeks. The TOAs are eventually fit to a parameterized model and the timing residuals can be analysed further. The data we receive from the pulsar. Each pulsar has its own signature pulse shape which fluctuates a lot between two consecutive rotations but when we fold over hundreds of pulses the result we get is a pulse profile which is extremely stable and reproducible.

The standard method to determine the phase shift between the measured data and a template is a χ^2 fit in the frequency domain. The analysis is done in the frequency domain because in frequency domain, time shifting becomes multiplication by a complex exponential and this can be easily dealt with in the standard χ^2 fit procedure. The value of χ^2 is the goodness of fit statistic and the goal is to minimize this function.

The phase shift between $d(\phi)$ and $p(\phi)$ can be found by minimizing the function:

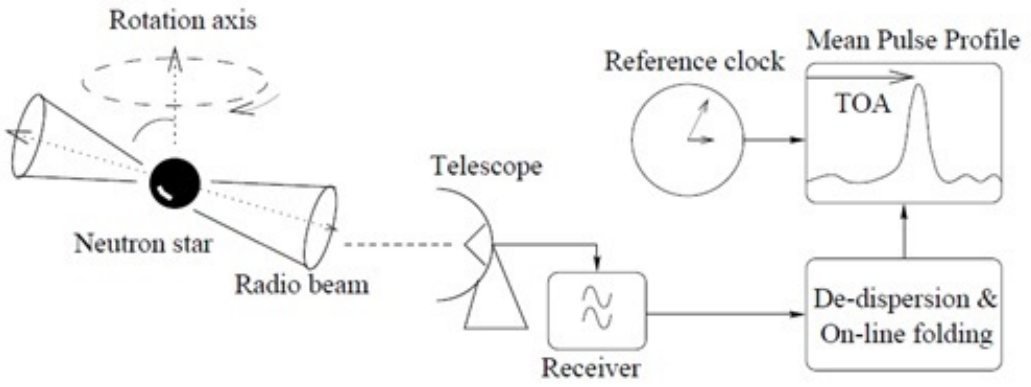

Figure 2.3: Schematic showing generation of pulse profile

$$\chi^2(a,\phi) = \sum_{k=1}^{k_{max}} \frac{|d_k - a p_k e^{-2\pi i k\phi}|^2}{\sigma_k^2} \tag{2.1}$$

where, $d_k = \sum_j d(j/N) e^{(-2\pi ijk/N)}$ is the Discrete Fourier Transform (DFT) of $d(\phi)$. p_k is defined similarly. Amplitude(a) and Phase shift(ϕ) are the fit parameters, and, σ_k is the noise power in each frequency bin of the DFT. For white noise, σ_k is a constant (Flat PSD). So, we can find $\Delta^2 = \sigma^2\chi^2$ and minimize this function. The absolute square can be multiplied out and we get the formula:

$$\Delta^2(a,\phi) = \sum_k |d_k|^2 + a^2 \sum_k |p_k|^2 - 2aR \sum_k d_k p_k^* e^{2\pi ik\phi} \tag{2.2}$$

$$= D^2 + a^2 P^2 - 2aC_{dp}(\phi) \tag{2.3}$$

where, $D^2 = \sum_k |d_k|^2$ and $P^2 = \sum_k |p_k|^2$ are the total power in each signal. All the phase information is contained in the term $C_{dp}(\phi) = R\sum_k d_k p_k^* e^{2\pi ik\phi}$ so maximizing C_{dp} will minimize Δ^2 and gives us the best fit $\phi = \hat{\phi}$ for a given value of a.

2.3 Dispersion Effects

High energy charged particles excite beams of radiation with a steep, negative slope radio spectrum upon being accelerated to relativistic energies out of the polar caps of the neutron stars. These pulses propagate through the ionized interstellar medium (ISM) where they undergo dispersion. The frequency dependent refractive index of the ISM disperses the pulses in such a way that lower frequencies will have a reduced group velocity and will arrive at the telescope later than higher frequency components. The dispersion is taken into account and is corrected for the dispersion by shifting the received signal by a certain amount.

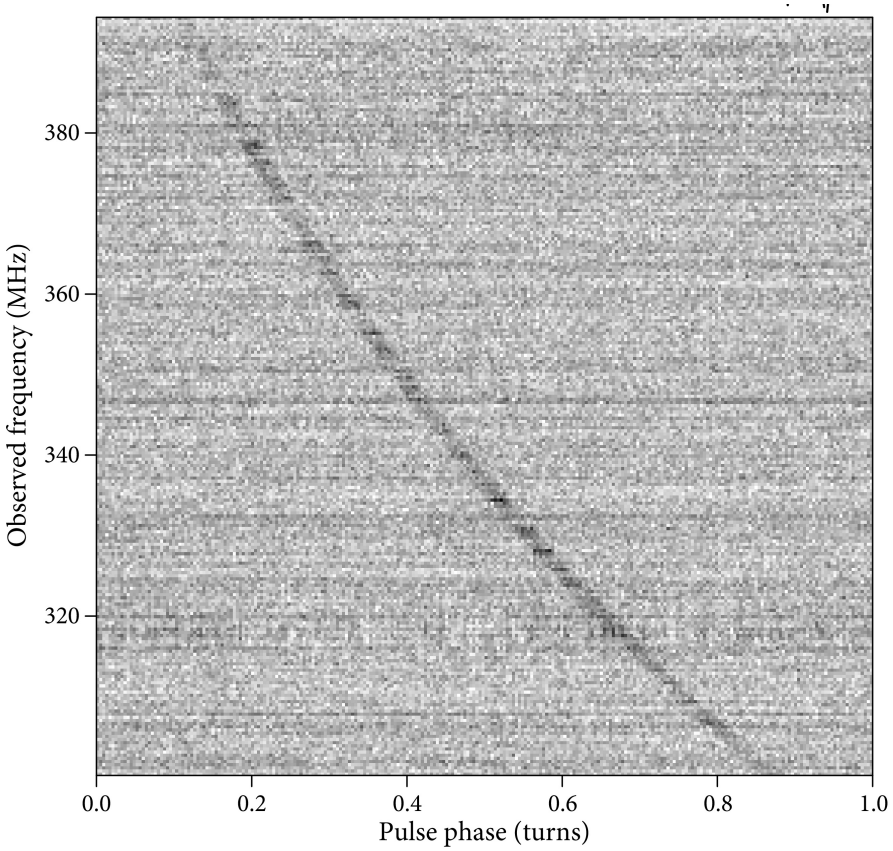

Figure 2.4: Pulsar dispersion. The gray scale shows the uncorrected dispersive delay as a function of frequency from an observation of the recently discovered pulsar J1400++50

Chapter 3

Gravitational Waves

Gravitational waves are ripples in space-time travelling at the speed of light. They provide new means for studying of black holes and the violent events that shape our universe. They can address questions pertaining to the assembly structure of galactic structures and the dynamical behaviour of gravitational fields. The theoretical possibility of gravitational radiation was recognized soon after the formulation of Einstein's general theory of relativity. It is easy to show that the Einstein's equations permit freely propagating wave solutions.

3.1 Linearized Gravity

Linearized gravity is an approximation to the solution of einstein's equation in which the nonlinear contributions in the metric are ignored. We look for small perturbations in the minkowski metric given as

$$g_{\mu\nu} = \eta_{\mu\nu} + h_{\mu\nu} \tag{3.1}$$

where, $|h_{\mu\nu}| << 1$. The frame-invariant distance between space-time events at the points x^μ and $x^\mu + dx^\mu$ is given by

$$ds^2 = dx^\mu dx_\mu = g_{\mu\nu} dx^\mu dx^\nu \tag{3.2}$$

The metric tensor describes the action of gravity through the statement that any particle which is free of the influence of other forces move through space time along a geodesic. Using the metric tensor in the equation 3.1 leads to the linearized Einstein's equation:

$$\partial_\mu \partial^\mu (h_{\mu\nu} - \frac{1}{2} n_{\mu\nu} h^\alpha_\alpha) = -16\pi T_{\mu\nu} \tag{3.3}$$

Here $T_{\mu\nu}$ is the stress-energy tensor, which gives the description of the density and momentum at each point in space time. The freely propagating wave equations can be obtained by setting $T_{\mu\nu} = 0$, which reduces the equation (of Einstein's equation) to the simple homogeneous wave equation. There is a gauge freedom in determining h since only derivative terms appear in both the equations. For a plane wave travelling in a given direction, there are only two physical degrees of freedom (polarizations) in h. The usual gauge choice is called the "transverse-trace-less" gauge in which the plane wave travelling in the z direction is represented by:

$$h_{\mu\nu}^{TT} = A_{\mu\nu} e^{ik_i x^i} \tag{3.4}$$

where,

$$A_{\mu\nu} = A_+ e_{\mu\nu}^+ + A_\times e_{\mu\nu}^\times = \begin{bmatrix} 0 & 0 & 0 & 0 \\ 0 & A_+ & A_\times & 0 \\ 0 & A_\times & -A_+ & 0 \\ 0 & 0 & 0 & 0 \end{bmatrix} \tag{3.5}$$

and, A_+ and $A_\times$ give the amplitudes of the two polarizations, usually called the "plus" and "cross" polarizations respectively. These are represented by the basis tensors $e_{\mu\nu}^{+,\times}$. The equations also require $k_\mu k^\mu = 0$, which means that the waves travel at the speed of light, obeying $\omega = \mathrm{k}$, exactly the same as electromagnetic radiation.

The corresponding figures in figure 3.1 shows the effect of both polarizations on an initially circular ring of particles, oriented transverse to the wave propagation direction.

3.2 Evidence for Gravitational Waves

The discovery of pulsar PSR B1913 + 16, a pulsar with a companion neutron star by Hulse and Taylor in 1974 was the first instance where compact objects in a binary system could be observed. Hulse and Taylor claimed that the binary should be emitting GWs and that consequently the binary's orbital period would shrink due to energy loss from gravitational radiation. The orbit was demonstrated to be decaying exactly as that claimed by the theoretical prediction as shown in figure 4. This was the first indirect detection of gravitational waves.

The first direct detection of gravitational waves. On February 11, 2016, the LIGO Scientific Collaboration and Virgo Collaboration announced the first confirmed observation of gravitational waves from colliding black holes. The gravitational wave signals were observed by the LIGO's twin observatories on September 14, 2015 and are shown in Figure 3.3. The time delay between the signal at Livingston and Hanford also confirmed that GWs propagate at the speed of light.

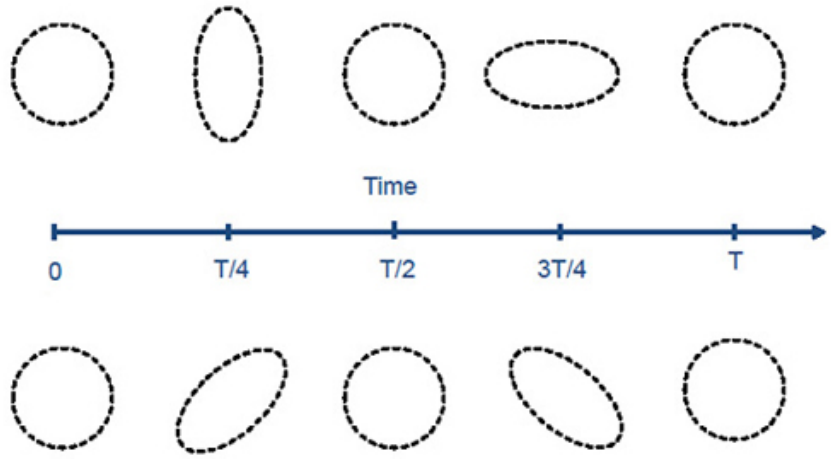

Figure 3.1: Upper diagram: For free masses initially arranged in a circle, a gravitational wave travelling into the page with a period, T, stretches and then compresses space along the vertical axis and vice versa along the horizontal axis. This is called the "+" polarization state of the wave. Lower diagram: The "×" polarization state stretches and compresses space along axes tilted 45

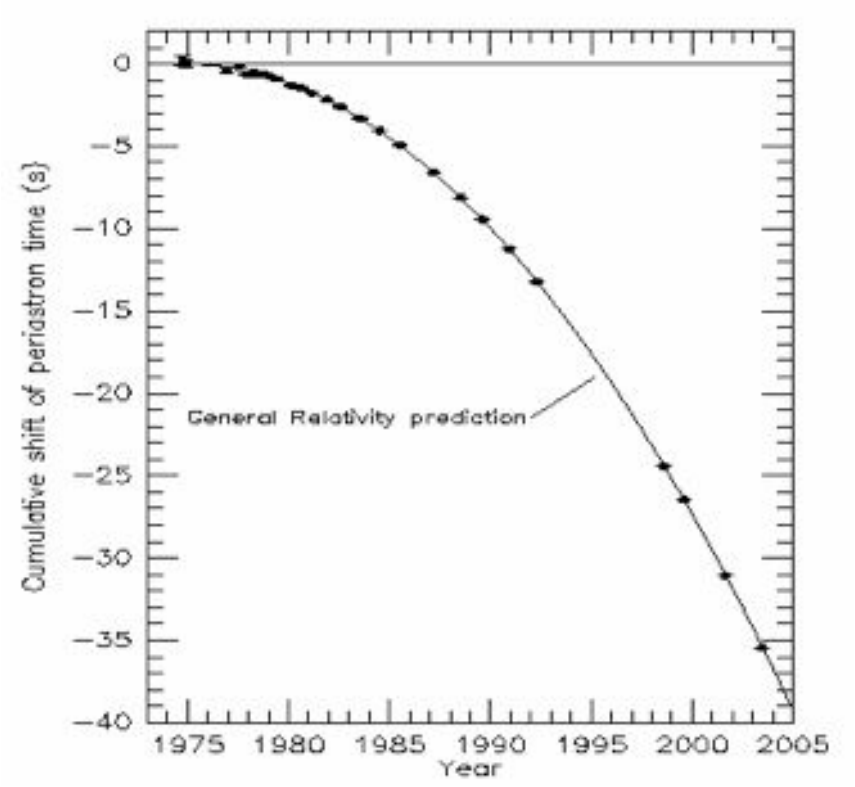

Figure 3.2: The graph showing a perfect correlation between observed and predicted values for the binary pulsar system

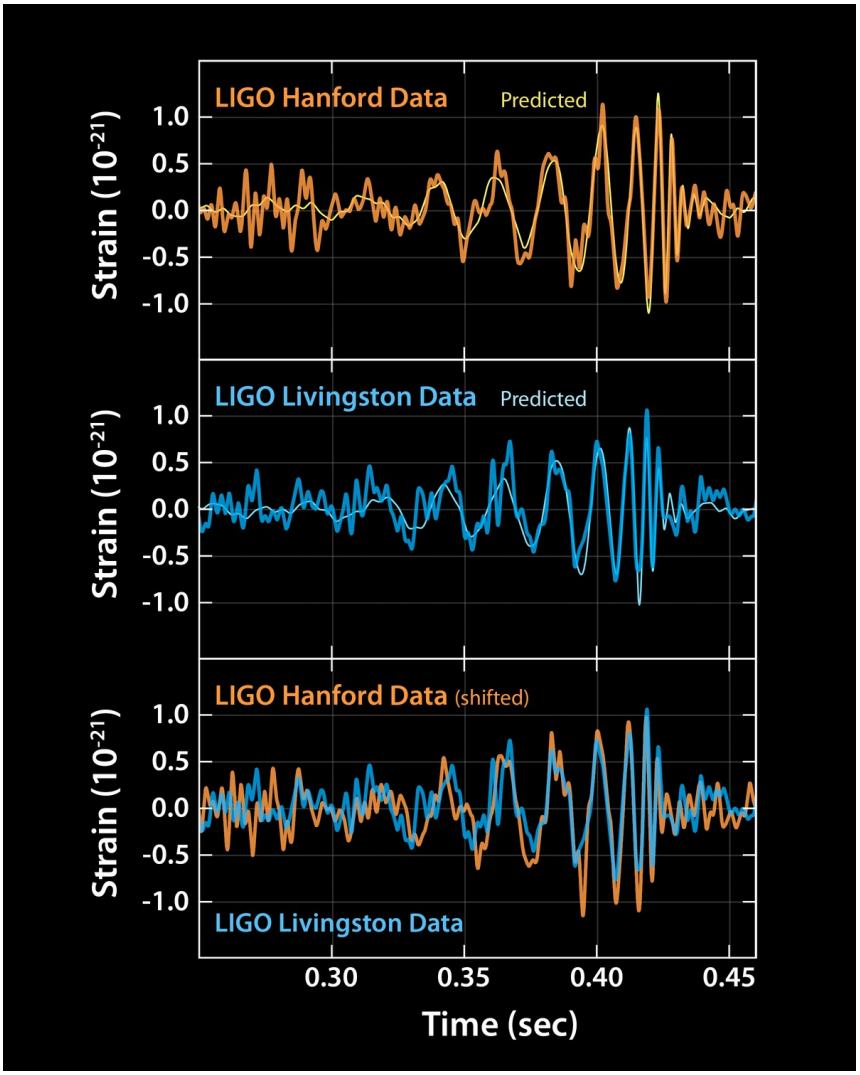

Figure 3.3: LIGO Detection

3.3 Types of Gravitational Waves

There are four main sources of gravitational waves caused by different kinds of motion and changing distributions of mass continuous, inspiral, burst, and stochastic.

1. *Continuous sources* - Continuous gravitational waves can be produced by systems that have a fairly constant and well- defined frequency. A spinning source can emit gravitational waves at a constant rate if it has bumps or imperfections in its shape. So if the spinning stays constant, the gravitational waves also remain continuous and have the same amplitude and frequency. Example of a continuous gravitational wave source would be a dense star like a neutron with imperfections on its surface.

2. *Inspiral* - As the name implies, these kind of gravitational waves are generated during the end of life stage of binary systems in which the two massive objects are spiralling into each other. The orbital distance decreases and their speeds increase due to the conservation of angular momentum. This causes the frequency of the gravitational waves to increase until the moment they coalesce.

3. *Stochastic* - There are many small gravitational waves passing by in the Universe all the time and they are mixed together. These gravitational waves are small in amplitude and are random. They are called stochastic as they have a random pattern but they cannot be predicted in a precise manner.

4. *Burst* - They are gravitational waves which do not have a particular pattern and come for short duration from unanticipated sources. There are hypotheses that the source of these waves would be supernovae or gamma ray bursts.

Chapter 4

Pulsar Timing Arrays

Pulsar Timing Array (PTA) is a network of one or more radio telescope which regularly monitor millisecond pulsars. PTAs are gravitational wave detectors that span our galaxy and one of their main goals is to detect gravitational waves. Currently PTAs are the only way to search for GWs in the nanohertz-microhertz band. The basic principle of working is to measure the various time of arrival of different pulsars and to use the correlation in their variations to detect gravitational waves. The basic data acquired and analyzed by the PTAs are timing residuals as described before. These data points are built over long observation of each pulsar and are typically averaged over tens of thousands of rotation. They are averaged over such a long period so that they are relatively stable, precise and of significant signal to noise ratio (SNR). The typical durations of measurement using current telescopes is approximately about an hour. The frequency sensitivity is set by observing interruptions in a pulsar which is about three weeks. The total span of data is about thirty years as precision timing was started in the 1980s. Hence from this we can get the sensitivity range of $T^{-1} \leq f \leq C^{-1}$ which is generally quoted as a sensitivity in the nanohertz-microhertz regime.

The predicted arrival of time of a pulse is built from a defined model of the pulsar's rotation and so some of the GW power can be absorbed in the process. However since most intrinsic parameters of pulsars differ, the PTAs only generally suffer sensitivity losses at frequencies of 6 months or one year due to positional and parallax errors.

Another general figure is the root mean squared of the timing residuals, σ_n, which is typically $\leq 1\ \mu s$ for pulsars included in the PTAs.

4.1 Gravitational Wave detection using pulsar timing arrays

The varying $g_{\mu\nu}$ along the line of the sight path from a pulsar to Earth will either advance or retard the measured pulse time of arrival by changing the pulse's time of flight. If the delay is a changing function of time, it can

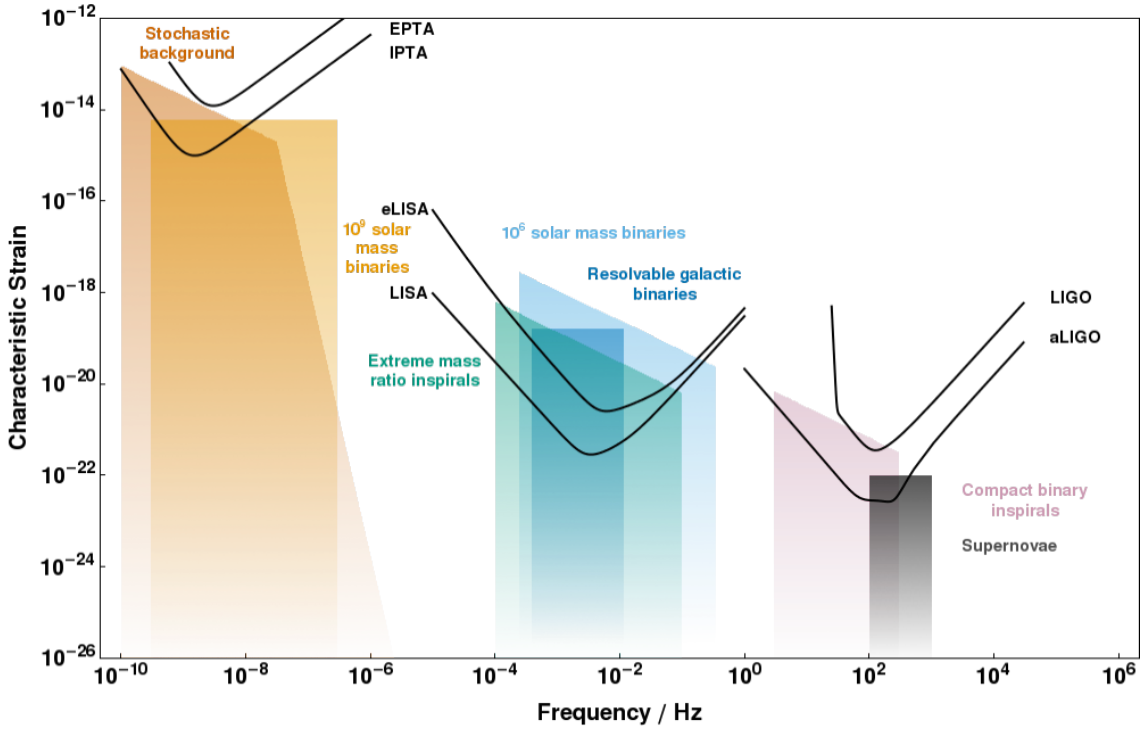

Figure 4.1: Noise curves for a selection of gravitational-wave detectors as a function of frequency.The characteristic strain of potential astrophysical sources are also shown. To be detectable the characteristic strain of a signal must be above the noise curve.

be detected as it will appear in the timing residuals. Photons travel along null geodesics, whose invariant length is 0. Thus using this information and combining it with equation 3.2 and the form of $g_{\mu\nu}$ given in 3.1 we get:

$$0 = ds^2 = dt^2 - dx^2 - h_{ij}dx_i dx_j \tag{4.1}$$

We can get the time of flight by solving this equation for dt and then integrating it along the flat space from the pulsar to earth. If we consider Earth to be at origin, the pulsar is at a distance d along the direction $\hat{n}$, and the pulse arrives at time to, then the path can be parameterized as $x_i(r) = (d-r)n_i, t(r) = t_0 + r - d$, and the time of flight can be written as:

$$T = \int dt = \int_0^d (\frac{dx_i}{dr}\frac{dx_i}{dr} + h_{ij}\frac{dx_i}{dr}\frac{dx_j}{dr})^{1/2}dr \tag{4.2}$$

$$= \int_0^d (1 - h_{ij}n_i n_j)^{1/2} \tag{4.3}$$

$$= d - \frac{1}{2}n_i n_j \int_0^d h_{ij}dr + o(h^2) \tag{4.4}$$

This gives us the total time of flight. We know that d is just the time of flight in flat space. So we can get the value of the deviation by subtracting this value from the above equation:

$$\Delta = T - d = \frac{1}{2} n_i n_j \int_0^d h_{ij} dr \tag{4.5}$$

We also know that $h_{ij}(x_i, t)$ satisfies the wave equation. A wave solution can be represented as a superposition of plane waves.

$$h_{ij}(x_i, t) = \int h_{ij}(\boldsymbol{k}) e^{ikt - ik_i x_i} d^3\boldsymbol{k} \tag{4.6}$$

Here $h_{ij}(\boldsymbol{k})$ is the amplitude of the wave propagating in the $\hat{\boldsymbol{k}}$ direction with the angular frequency k. It should be noted that there are only two freely adjustable components of each $h_{ij}(\boldsymbol{k})$. Also $h_{ij}(\boldsymbol{k})$ is not dimensionless and has dimensions of L^3. Combining equations 4.5 and 4.6 to get the following expression for Δ:

$$\Delta = \frac{i}{2} n_i n_j \int d^3\boldsymbol{k} h_{ij}(\boldsymbol{k}) \frac{(e^{ikt_0} - e^{ik(t_0 - d) - ik_i n_i d})}{k + k_i n_i} \tag{4.7}$$

The equation 4.2 describes the the contributions of an arbitrary collection of plane waves on the TOAs of a given pulsar. The first terms in the parentheses represent the wave phase evaluated at the Earth which is at the time of pulse reception. The second term represents the wave phase evaluated at the pulsar at the time of emission. The result shows that Δ is not only dependent on the metric tensor of the Earth but also on the weighted sum of all the incident plane waves. The above equation can also be written in terms showing the polarization dependence:

$$\Delta = \frac{i}{2} \int d^3\boldsymbol{k} \frac{1}{k} (\alpha_+(\hat{\boldsymbol{k}}, \hat{\boldsymbol{n}}) A_+(\boldsymbol{k}) + \alpha_\times(\hat{\boldsymbol{k}}, \hat{\boldsymbol{n}}) A_\times(\boldsymbol{k}))(1 - e^{-ikd - ik_i n_i d}) e^{ikt_0} \tag{4.8}$$

In this equation, $h_{ij}(\boldsymbol{k})$ is separated into its two polarization components. The formula depends on the implicit definitions of the polarization directions. Each of the polarization terms is split into its $A_{+,\times}$ and angular factor $\alpha_{+,\times}$. The angular factors depend on the the directions $\hat{\boldsymbol{k}}$, $\hat{\boldsymbol{n}}$ and the implicit polarization directions. They are defined as:

$$\alpha_{+,\times}(\hat{\boldsymbol{k}}, \hat{\boldsymbol{n}}) = \frac{n_j e^{+,\times}_{jk}(\hat{\boldsymbol{k}}) n_k}{1 + \hat{k}_i n_i} \tag{4.9}$$

This is the derivation of the effect that a set of gravitational waves will have on a set of gravitational waves on a radio pulse's time of flight from pulsar to Earth. These time deviations can be measured and the PTAs can be used as GW detector. There are also other effects that can cause similar deviations. The dominant effect is the contribution from the pulsar's translational and rotational of the pulsar itself, relative to Earth. These effects can be put together and a timing model of a given pulsar can be created. The form of the timing model is as follows:

$$\phi(t) = \phi_0 + \upsilon t + \frac{1}{2}\dot{\upsilon}t^2 + \frac{\upsilon}{c}|\boldsymbol{r}_p - \boldsymbol{r}_e| + ... \tag{4.10}$$

Here, υ is the intrinsic spin frequency, $\dot{\upsilon}$ is the spindown rate, and $\boldsymbol{r_p}$ and $\boldsymbol{r_e}$ are the position vectors to the pulsar and earth relative to an inertial reference frame. There are also additional terms which are not mentioned such as the description of orbital motion of pulsar, relativistic delays due to pulsar system and relativistic delays due to Solar system masses. We know the motion of the Earth through the Solar system with a high accuracy, but the pulsar's motion and location is determined straight from the timing measurements. This can be determined by using a χ^2 fit for the data as mentioned before. Owing to such errors, a single pulsar cannot make a definite detection of gravitational waves. The effect of a GW cannot be distinguished from these other deviations by a single pulsar. However, by continued measuring of an array of these millisecond pulsars, GWs can be detected by forming correlation of these timing residuals. The use of these correlations in finding GWs will be discussed in the next part.

4.2 Stochastic Background

The dominant source of GW at nHz frequencies is expected to be the mergers of supermassive black holes (SMBHs) that occur throughout the history of the Universe. In the nHz frequency range, the PTAs are sensitive to the stochastic background created by the incoherent sum of many such events. The resulting $h_{ij}(\boldsymbol{k})$ is expected to be uniform as a function of angle and have a red power-law spectrum.

We can form a $h_{ij}(\boldsymbol{k})$ by summing over all SMBH binary systems:

$$h_{ij}(\boldsymbol{k}) = \sum_{n=1}^{N_{BH}} A_n e^{i\phi_n}\big(e_{ij}^{+}(\hat{\boldsymbol{k}_n})cos2\theta_n + e_{ij}^{\times}(\hat{\boldsymbol{k}_n})sin2\theta_n\big)\delta(\boldsymbol{k} - \boldsymbol{k_n}) \tag{4.11}$$

Each of the binary units have a strength of A_n , an apparent frequency of k_n and come from direction $\hat{\boldsymbol{k}_n}$. The polarization (θ_n) and phase (ϕ_n) angles depend on the orientation of the system. The above equation 4.11 is based on several assumptions. We assume that the binary system's orbital

frequency is fixed, since the binary's evolution timescale is much longer than the observation time. Secondly, the systems have been assumed to be in circular orbits, which makes their GW emission monochromatic. We have also made the assumption that all the GW sources are far enough that their emission can be treated as plane waves.

For a stochastic approach, the expectation value can be calculated and simplified as was done by Jaffe and Backer([1]). Each system in the sum has parameters which are drawn randomly from a probability distribution $p(A, k)$. All angular parameters are take to be uniformly distributed. Using this approach, we can get the expectation value:

$$\frac{1}{2}E\{h^*_{ij}(\boldsymbol{k})h_{ij}(\boldsymbol{k}')\} = N_{BH}\frac{\delta(\boldsymbol{k}-\boldsymbol{k}')}{4\pi k^2}\int A^2 p(A,k)dA = \frac{\delta(\boldsymbol{k}-\boldsymbol{k}')}{4\pi k^2}S_h(k) \tag{4.12}$$

The equation 4.12 defines the Strain power spectrum $S_h(k)$, which has units of inverse frequency. The characteristic strain h_c is related to this as $h_c(k) = \sqrt{kS_h(k)}$. The experimental limits on the stochastic background is generally written in terms of h_c since it is directly measurable and the units of frequency cancel out, leaving a dimensionless number that characterizes the strain amplitude.

The key result of Jaffe and Backer ([1]) is the prediction of a GW spectrum that has the shape $h_c \propto \upsilon^{-2/3}$, and an amplitude A $\approx 10^{-15}$ at $\upsilon = 1yr^{-1}$. The spectral slope of $-2/3$ has a robust result and has been noted by other authors also. The slope comes from two basic formulae regarding gravitational radiation from binary systems (e.g Peters and Mathews [20];Misner et al) ([21]). As the binary loses energy to GW, the orbit decays and this increases the GW frequency. The system radiates more intensely at the high frequency era of its life, however it spends more time radiating at lower frequencies.

Dynamical friction refers to the gravitational interactions between the binary system and other bodies. This dynamical friction is necessary to reduce the size of the binary to a point where significant GW can be generated as it tend to remove energy from the binary (reference). However as long as the dominant energy loss mechanism is dynamical friction rather than GW, we will not observe any GW from the system. The frequency at which GW emission takes over dynamical friction will be the lowest observed GW frequency. The low frequency cut-off for this is estimated to be $10^{-4} - 10^{-2}$ yr^{-1} by (reference) for many types of galaxy. A cutoff value much higher than this would reduce the likelihood of pulsar GW detection. Given a long enough data span, the spectrum could potentially be observed or at least constrained using pulsar data.

We can see the effect of a stochastic background on pulsar timing measurements by combining 4.8 and 4.11 as follows:

$$\Delta(t) = \sum_n \frac{A_n e^{i\phi_n}}{2k_n}\big(\alpha_+(\hat{\boldsymbol{k}_n}, \hat{\boldsymbol{n}})cos2\theta_n + \alpha_\times(\hat{\boldsymbol{k}_n}, \hat{\boldsymbol{n}})sin2\theta_n\big)(1 - e^{-ik_n d - ik_i n_i d})e^{ik_n t} \tag{4.13}$$

In the frequency domain $\Delta(\omega)$ has exactly the same form as given in equation 4.13 with the final exponential $e^{ik_n t}$ replaced by $\delta(\omega - k_n)$. This result is not only true for a background of SMBHs but the equations are applicable to any set of sources that can be expressed as a sum of oscillators.

4.3 Measurement using several Pulsars

We can use equations 4.8, 4.9 and 4.12 to compute the expected cross correlation between two sets of timing data:

$$\rho(\tau) = E\{\Delta_1(t_0 - \tau)\Delta_2(t_0)\} \tag{4.14}$$

$$= N_{BH}\int \frac{A^2}{8k^2}p(A,k)\gamma(\hat{\boldsymbol{k}}, \hat{\boldsymbol{n}_1}, \hat{\boldsymbol{n}_2})\big(1 - e^{ikd_1(1+\mu_1)}\big)\big(1 - e^{ikd_2(1+\mu_2)}\big)e^{ik\tau}\frac{dAd^3\boldsymbol{k}}{4\pi k^2} \tag{4.15}$$

Here, Δ_1 and Δ_2 are the timing fluctuations for two pulsars, which are located at the positions $d_1\hat{\boldsymbol{n}_1}$ and $d_2\hat{\boldsymbol{n}_2}$ relative to Earth. μ_1 and μ_2 are defined as $\hat{\boldsymbol{k}} \cdot \hat{\boldsymbol{n}_1}$ and $\hat{\boldsymbol{k}} \cdot \hat{\boldsymbol{n}_2}$ respectively. The angular factor γ is a function of the orientation of $\boldsymbol{k}$ and the pulsar directions. It is given as:

$$\gamma(\hat{\boldsymbol{k}_n}, \hat{\boldsymbol{n}_1}, \hat{\boldsymbol{n}_2}) = \alpha_+(\hat{\boldsymbol{k}}, \hat{\boldsymbol{n}_1})\alpha_+(\hat{\boldsymbol{k}}, \hat{\boldsymbol{n}_2}) + \alpha_\times(\hat{\boldsymbol{k}}, \hat{\boldsymbol{n}_1})\alpha_\times(\hat{\boldsymbol{k}}, \hat{\boldsymbol{n}_2}) \tag{4.16}$$

When the terms inside the parentheses in equation 4.14 is expanded, we get four terms. Three of these terms contain rapidly oscillating exponentials (since $kd >> 1$). These will average out when the integral is performed. The term responsible for correlation is the first constant term. It represents the contribution from the Earth end of the time shift integral for each pulsar. The three oscillatory terms can be dropped, and the angular and radial parts separate as follows:

$$\rho(\tau) = \frac{N_{BH}}{8}\int A^2 p(A,k)e^{ik\tau}dAdk \int \gamma(\hat{\boldsymbol{k}}, \hat{\boldsymbol{n}_1}, \hat{\boldsymbol{n}_2})\frac{d\Omega_k}{4\pi} \tag{4.17}$$

The angular integral is much more complicated than the radial part and will result in the expected correlation between the two sets of time shifts depending on the angular separation of the two pulsars. The cross correlation function can be written as:

$$\rho_{12}(\tau) = \frac{1}{2} C_\Delta(\tau)\zeta(\beta_{12}) \tag{4.18}$$

where, C_Δ is auto-correlation function which can be solved by evaluating the radial part of the integral and $\zeta(\beta)$ is the angular function in which $\beta \equiv \hat{\boldsymbol{n}}_1 \cdot \hat{\boldsymbol{n}}_1$ is the cosine of angular separation between $1-2$. An evaluation of the angular integral was performed by Hellings and Downs ([4]), giving the following results.

$$\frac{\zeta(\beta)}{3} = \frac{1-\beta}{1} log(\frac{1-\beta}{2}) - \frac{1-\beta}{12} + \frac{1}{3} \tag{4.19}$$

This function is plotted in figure . This demonstrates the correlation of the timing residuals of the two pulsars with the angular separation between the two pulsars. If this correlation is detected between two pulsar, it would result in an unambiguous detection of GW. This method of combining data from many pulsars is used for gravity detection in a pulsar timing array.

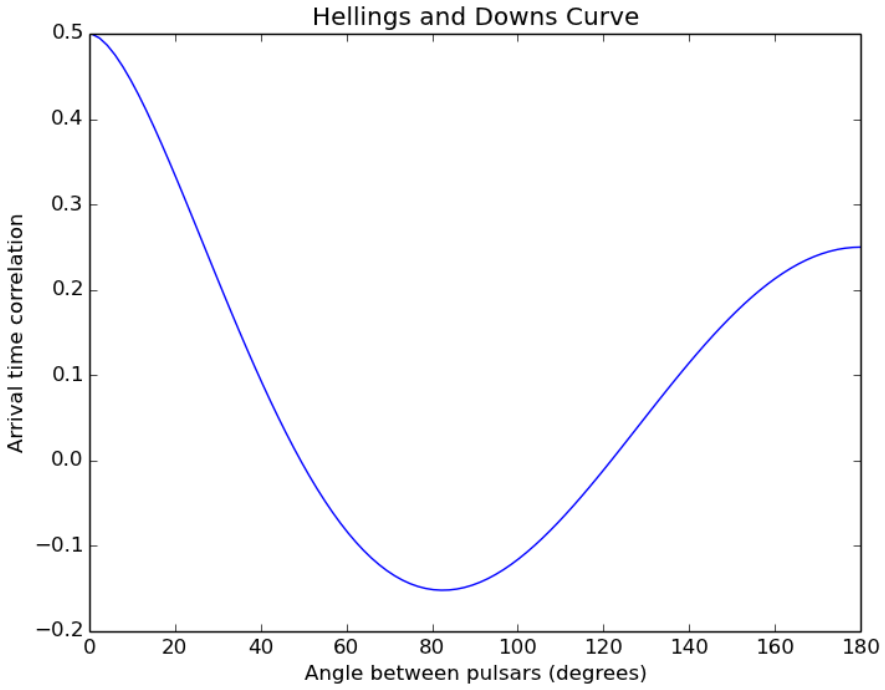

Figure 4.2: Hellings and Downs curve: Showing the correlation between angular separation of two pulsars and time correlation

Till now, none of the pulsar groups have seen any correlation in their data, just noise. If a fit of this curve is observed and the results are statistically significant then a gravitational wave would be detected. This would be a gradual process with the points moving slowly over time from noise to a good fit.

4.4 Continuous Waves

The current focus of PTA searches is to uncover evidence for nanohertz stochastic gravitational wave background, which is most likely composed of many overlapping inspiraling supermassive black hole(SMBH) binary signals. This background dominates at the lowest detectable frequencies while at higher frequencies the signals become less stochastic and single bright sources rise above the stochastic signal becoming the dominant signal. Numerous studies have shown that these massive nearby binary systems may be bright enough to resolve with PTAs, thus presenting an opportunity to probe the early inspiral regime of their coalescence. For an inspiraling circular binary of component masses m_1 and m_2, the GW strain amplitude is given by [24]:

$$h_0 = 2\frac{(GM_c)^{2/3}}{c^4}\frac{(\pi f)^{2/3}}{d_L} \tag{4.20}$$

where, d_L is the luminosity distance of the source, and M_c is their chirp mass which s define as $M_c = M\eta^{5/3}$, with $M = m_1 + m_2$ and $\eta = \frac{m_1 m_2}{M^2}$ the symmetric mass ratio.

4.5 Gravitational wave bursts

There are potential sources of burst sources which can be potential detected by PTAs such as the formation or coalescence of supermassive black holes, the passage of massive compact objects in unbound orbits around a supermassive black hole, cosmic string kusps or kinks. However, there have been no published results to impose limits on these bursts using real data.

Chapter 5

Developments

The sensitivity of a PTA depends upon the type of the target signal. However, there are other factors that can improve this sensitivity. Minimizing the pulsar's σ_n, reducing the presence of noise in the timing residuals and minimizing the sampling intervals for higher frequencies while maximizing the total span of data, the and the number of millisecond pulsars. There have been several coordinated efforts for pulsar timing arrays and there is a push for combining the data to form an international effort. Some of the leading programs are:

The North American Nanohertz Observatory for Gravitational Waves (NANOGrav) has been running for over a decade and is currently using the Green Bank and Arecibo telescopes to time 43 pulsars. each of the pulsars are observed 327 MHz and 2.3 GHz. The reason for the bi-frequency is to mitigate the effects of the interstellar medium on the timing residuals.

The European Pulsar Timing Array (EPTA) is a collaboration which uses five telescopes across Europe - Effelsberg, Lovell, Nancay, Sardinia, and Westerbork and they separately time a primary set of 41 pulsars at various frequency pairs between 300 MHz and 3.5 GHz. Because five telescopes contribute independently to EPTA data, it has the highest cadence of the three PTAs, effectively having one data point per pulsar each week.

The Parkes Pulsar Timing Array (PPTA) times 25 pulsars using Parkes Observatory in Australia at frequencies of 600 MHz, 1.5 GHz, and 3 GHz. This experiment is unique due to the telescope's position in the southern hemisphere so it can see a distinct set of pulsars which are not visible to the EPTA nor NANOGrav. The PPTA has continually boasted the best constraints on gravitational radiation since it has one of the best timed pulsars in the sky, PSR J0437-4715 (Hobbs et al. 2010)

The International Pulsar Timing Array (IPTA) represents the coordinated effort to combine data from the above three projects to reach the best possible sensitivity to GWs . For its initial 2015 data release, the array contains a total of 49 pulsars. This number is not the sum of the above collaboration's pulsars because the PTAs do not time mutually exclusive pulsars, and the 2015 IPTA data release does not contain pulsars that have

been added to the constituent arrays in only the last few years.

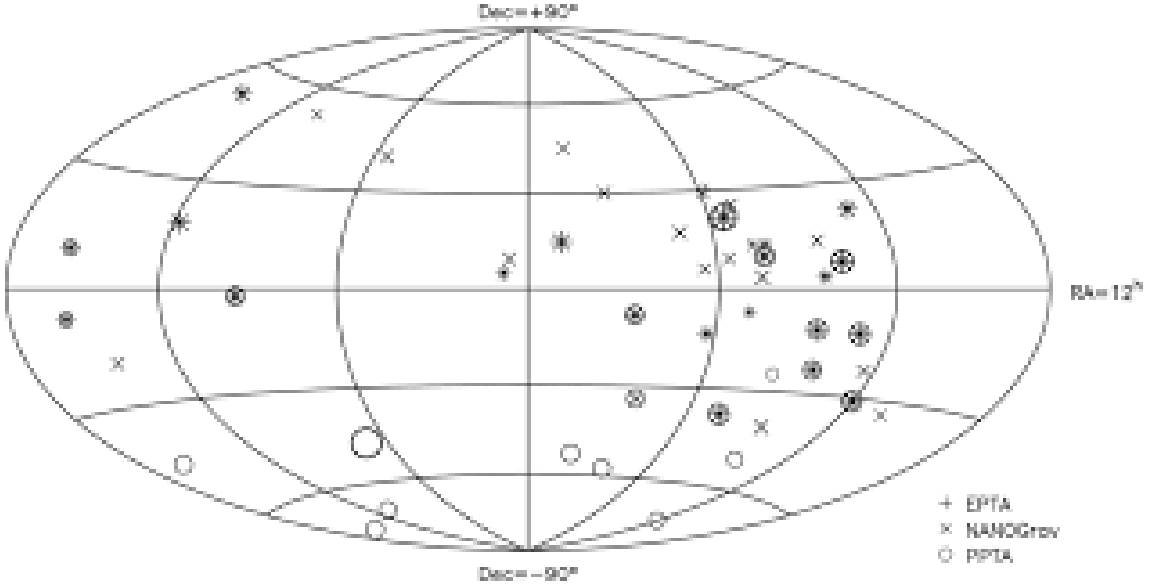

Figure 5.1: Distribution on the sky of the pulsars being observed by participating PTAs.

5.1 The search for new pulsars

Finding many pulsars that can be timed to low σ_n is another important part of increasing PTA sensitivity. Only a few low σ_n pulsars contribute significantly to the PTAs. Millisecond pulsars (MSPs) with rotational frequencies of hundreds of Hz are the only pulsars stable enough for PTA use, and there are ongoing worldwide efforts to find more of these pulsars. This has turned up 20-30 new millisecond pulsars per year in the last 6 year although only five of these are suitable for PTA use. The wealth of potential MSPs will become observable with future telescopes and large cllecting area like the Square Kilometre Array (SKA). Adding these pulsars would increase our sensitivty to GWs.

Chapter 6

Conclusion

Pulsar timing is a complementary method for gravitational waves. Pulsar Timing Arrays have reached unprecedented sensitivities and have started to put constraints on the cosmic population of supermassive black hole mergers by detecting the gravitational wave background. They are currently used to constrain galaxy formation models by providing these limits. Gravitational detections require cross correlations to simultaneously analyze timing residuals from multiple pulsars. The timing sensitivity to GW is impacted by the radio telescope sensitivty, the number of good timing pulsars and timing noise. With better telsecopes, a wider range of these pulsars can be observed and so the earliest expected detection could arrive in a few years. PTAs also contribute fundamentally to other areas of study and have also been used to create a pan- galactic pulsar based timescale. The coming years, this ongoing timing of pulsars will eventually drive PTA science from "beginning to impact our knowledge of the Universe" to "measuring the structure and evolution of the Universe."

References

[1] Coalescence Rate of Black Hole Binaries, http://iopscience.iop.org/article/10.1086/345443/fulltext/55620.text.html

[2] Stanislav Babak et. al., European Pulsar Timing Array Limits on Continuous Gravitational Waves from Individual Supermassive Black Hole Binaries>, https://arxiv.org/abs/1509.02165

[3] V. Ravi, Prospects for gravitational-wave detection and supermassive black hole astrophysics with pulsar timing arrays, https://arxiv.org/abs/1406.5297

[4] Hellings, Downs, Upper limits on the isotropic gravitational radiation background from pulsar timing analysis http://adsabs.harvard.edu/abs/1983ApJ...265L..39H

[5] Pulsar timing noise and the minimum observation time to detect gravitational waves with pulsar timing arrays https://arxiv.org/abs/1310.4569

[6] Detecting nanohertz gravitational waves with pulsar timing arrays, https://arxiv.org/pdf/1509.06438.pdf

[7] Gravitational-Wave Detection and Astrophysics with Pulsar Timing Arrays, https://arxiv.org/pdf/1511.07869.pdf

[8] The International Pulsar Timing Array: A Galactic Scale Gravitational Wave Observatory, https://arxiv.org/abs/1409.4579

[9] http://www.ipta4gw.org/

[10] http://nanograv.org/research/

[11] http://science.sciencemag.org/content/sci/342/6156/334.full.pdf

[12] http://physicstoday.scitation.org/doi/full/10.1063/PT.3.3621

[13] The sensitivity of pulsar timing arrays https://arxiv.org/pdf/1408.0739.pdf

[14] Constraints on Individual Supermassive Black Hole Binaries from Pulsar Timing Array Limits on Continuous Gravitational Waves https://arxiv.org/pdf/1510.08472.pdf

[15] Detection and localization of continuous gravitational waves with pulsar timing arrays: the role of pulsar terms https://arxiv.org/pdf/1606.04539.pdf

[16] https://medium.com/starts-with-a-bang/mysteriously-quiet-space-baffles-researchers-c9ba6220e943

[17] Noise in pulsar timing arrays https://arxiv.org/abs/1505.00402

[18] Understanding the residual patterns of timing solutions of radio pulsars with a model of magnetic field oscillation https://arxiv.org/abs/1603.04998

[19] Detection of Gravitational Waves using Pulsar Timing https://arxiv.org/pdf/1004.3602.pdf

[20] Gravitational Radiation from Point Masses in a Keplerian Orbit Plane https://journals.aps.org/pr/abstract/10.1103/PhysRev.131.435

[21] Charles W. Misner & Kip Thorne, Gravitation, ISBN: 9780716703440

[22] Measuring the gravitational wave background using precision pulsar, https://arxiv.org/abs/0809.0791.

[23] Gravitational Wave detection & data analysis for Pulsar Timing Arrays https://gwic.ligo.org/thesisprize/2011/van_haasteren_thesis.pdf

[24] K. S. Thorne. in Hawking S., Israel W., eds, Three Hundred Years of Gravitation. Cambridge Uni. Press, Cambridge, 1987.